COMMUNICATION

Photoreversible formation of nanotubes in water from an amphiphilic azobenzene derivative

Received 00th January 20xx,
Accepted 00th January 20xx

DOI: 10.1039/x0xx00000x

Diego Navarro-Barreda, César A. Angulo-Pachón, Francisco Galindo and Juan Felipe Miravet*

An anionic azobenzene-appended derivative of L-ValylGlycine self-assembles into nanotubes in water. Irradiation with 365 nm light provokes *trans-cis* isomerization of the azobenzene unit and subsequent tube disassembly. Thermal or photoinduced (457 nm light) recovery of the *trans* isomer restores the nanotubes.

Responsive and adaptive organic molecular (nano)materials are used, among other fascinating applications, as actuators and in targeted drug release.[1–3] The use of light as a stimulus is especially attractive because it provides spatial and temporal control without direct contact. Thus, for example, controlled delivery of bioactive molecules in a given microenvironment with a good time and position resolution is of utmost interest for biomedical applications.[4,5]

Amphiphilic molecules are a preferred building block for preparing functional molecular materials in aqueous environments.[6] Particularly, photoresponsive amphiphiles afford materials whose formation and function are light-controlled.[7] Examples of units that can undergo light-induced reversible changes in their structure and that have been incorporated into amphiphiles include derivatives of diarylethene,[8] spiropyran[9] and, mostly, azobenzene.[10,11]

Azobenzenes show outstanding properties for their use as a photoswitch, such as excellent reversibility and *trans-cis* isomerization cycles endurance.[12,13] Photocontrollable self-assembly has been mainly studied using molecules with azobenzene moieties.[14] Examples include the formation or size regulation of micelles,[15] vesicles,[16–19] organic nanoparticles,[20,21] molecular hydrogels[22,23] and the reversible conversion between nanotubes and nanoparticles.[24] With a biomedical perspective, azobenzene isomerization permits photocontrol of complex biological systems,[25,26] and an azobenzene-modified diphenylalanine derivative has been used for photocontrolled targeted delivery of siRNA biomolecules.[27]

Peptide-derived nanotubes have received much attention focused on understanding their self-assembly mechanism and exciting properties.[28–30] Aside from cyclic peptides,[31] many of the studies on peptide nanotubes are based on the self-assembly of dipeptide derivatives. Remarkably, the diphenylalanine motif is prone to self-assemble into tubular structures, and many studies have been carried out in this direction.[32] Peptide nanotubes are studied in the context of different applications in areas such as electronics, sensors, and biomedical materials, among others.[33] Noticeably, peptidic nanostructures can be used for targeted drug delivery.[34,35]

Here we report on the light-controlled reversible formation of nanotubes from a derivative of L-ValGly with an appended azobenzene moiety (**SucValGlyAzo**, **Scheme 1**). Up to our knowledge, these results are unprecedented. In related work, a diphenylalanine moiety with a pendant azo-group formed fibrils that evolved to vesicles upon photoisomerization. [36] The insertion of an azobenzene moiety in a decapeptide permitted photoregulated fibrilization.[37] A diglycine-based molecule containing an azobenzene unit changed its aggregation upon irradiation from nanoribbons to a hydrogel.[38]

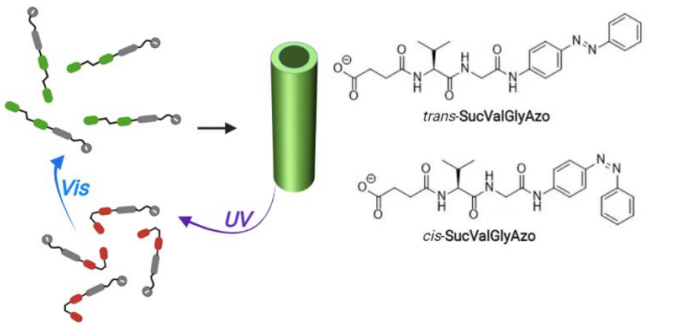

Scheme 1. Structure of **SucValGlyAzo** and pictorial representation of its photoisomerization and nanotube formation.

Departamento de Química Inorgánica y Orgánica, Universitat Jaume I, Av. Vicent Sos Baynat s/n. Castellón, 12071, Spain. E-mail: miravet@uji.es

†Electronic Supplementary Information (ESI) available: Experimental details, supplementary figures cited in the main text, characterization data. See DOI: 10.1039/x0xx00000x

SucValGlyAzo was prepared from L-ValGly by N-acylation with succinic anhydride at the N-terminus and amide formation with 4-aminoazobenzene at the C-terminus, using the corresponding N-protection and C-activation strategies (see SI for details). The introduction of a succinic acid moiety has been explored several times in our previous work to produce molecules that can aggregate in water to yield gels formed by fibrillar networks[39–41] or nanoparticles.[42]

SucValGlyAzo showed, as expected, a reversible *trans-cis* photoisomerization. **Fig. 1** shows that upon irradiation with UV light, the absorption band at ca. 340 nm diminishes in parallel with the increase of the band of the *cis*-isomer at ca. 440 nm. The measurements were carried out in tris(hydroxymethyl)aminomethane (Tris) buffer at pH 7.4, where the predominant species of **SucValGlyAzo** is the carboxylate (the pK_a of the conjugated acid is 6.1). The photoisomerization process was found to be fully reversible. Several cycles of *trans-cis* interconversion could be performed by alternative irradiation at 365 nm and 457 nm, without significant alteration of the chromophore (Fig. 1). As usual for the azobenzene unit, thermal energy also permits a progressive *cis-trans* transformation, which is significantly slower for this molecule. For example, the absorption spectrum of the *cis* isomer is almost unchanged after 10 minutes of thermal equilibration at 25 ºC. It requires more than one hour to recover the trans form (**Fig. S1**) fully. However, after irradiating the *cis* isomer with visible light, the *trans* form is obtained immediately. (**Fig. S2**).

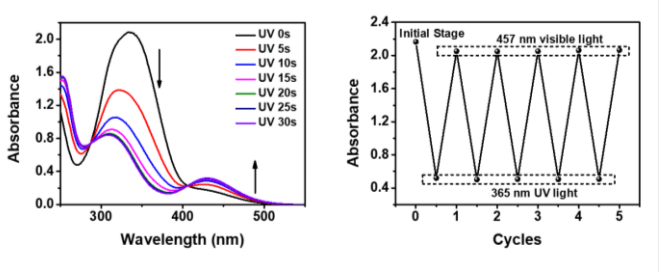

Fig. 1. Left: UV-Vis spectra of **SucValGlyAzo** as a function of time upon 365 nm UV light irradiation Right: Absorbance changes at 340 nm observed during five cycles of consecutive irradiation for 30 seconds with 365 nm UV light and 457 nm visible light. [**SucValGlyAzo**] = 1.7 mM, 0.1 M Tris buffer, pH 7.4, 25 ºC.

The aggregation of **SucValGlyAzo** was monitored by dynamic light scattering (DLS). The plot of the intensity of scattered light *vs.* concentration of the azo derivative reveals a scattering onset at ca. 0.6 mM, ascribable to the critical aggregation concentration (**Fig. 2**). The analysis of the size distribution obtained by DLS is also shown in Fig. 2. A broad distribution was obtained with an intensity averaged apparent diameter (Di) of 334 ± 49 nm and a polydispersity index (PdI) of 0.50 ± 0.09. Filtration through a 0.45 µm mesh nylon filter to remove large particles afforded a monomodal symmetrical size distribution, with Di = 107.0 ± 1.0 nm and PdI = 0.203 ± 0.012. The nanometric objects showed reasonable temporal stability, being the size distribution very similar after storage for 16 h of the sample at 4ºC (**Fig. S3**). It has to be noted that DLS results are commonly presented as a particle diameter distribution, obtained from the Stokes-Einstein equation assuming spherical particles.[43] However, for rods or cylindrical objects, as those described below, the analysis is much more complex.[44] For this reason, the plot in Fig. 2 shows the distribution of diffusion coefficients and the apparent diameter, namely, that obtained assuming spherical particles.

Given the anionic nature of **SucValGlyAzo** at neutral pH values, it was expected that its aggregation could be influenced by the concentration and nature of the cations present in the medium. For this reason, a comparison of dispersing media was made by DLS in 0.1 M Tris, phosphate (PB) and 4-(2-hydroxyethyl)-1-piperazineethanesulfonic acid (HEPES) buffers (**Fig. S4**). Significant differences were found. The sample in PB shows a broad bimodal distribution of sizes (D_i ca. 400 and 2000 nm). For the case of HEPES buffer, also a bimodal distribution of smaller objects is obtained (D_i ca. 40 and 200 nm). These results differ from the monomodal size distribution previously obtained for the aggregation of **SucValGlyAzo** in Tris (Fig. 2). Seemingly, the different characteristics of the cations present in the buffers affect the aggregation according to these preliminary assays, but further studies would be required taking into account variables such a pH or ionic strength. It is worth noting that PB contains mainly the spherical and relatively small cation sodium, which presumably promotes larger aggregated species. HEPES buffer preparation requires neutralization with sodium hydroxide, affording sodium and ammonium species as cations. However, Tris buffer contains exclusively organic ammonium-type cations. This behavior is directly related to the Hofmeister (lyotropic) series, where the sodium cation presents a significantly higher aggregation-promoting effect than ammonium derivatives.[45]

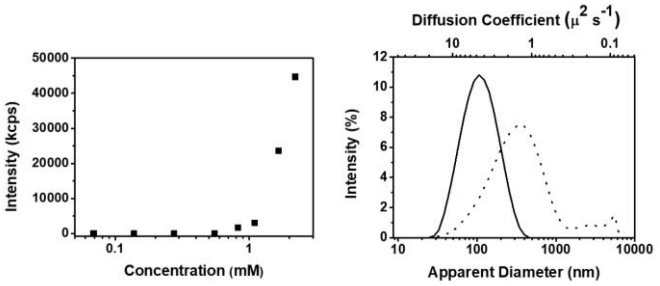

Fig. 2. Left: Variation of the intensity of scattered light with the concentration of **SucValGlyAzo** determined by DLS. Right: Diffusion coefficient and apparent diameter particle distribution determined by DLS for a 1.7 mM sample of **SucValGlyAzo** before (dashed line) and after (solid line) filtration through a 0.45 µm mesh filter. All the measurements were carried out in 0.1 M Tris buffer, pH 7.4, 25 ºC.

Electron microscopy revealed that the objects detected by DLS correspond to nanotubes. The images in Fig. 3 correspond to a sample treated with a 0.45 µm mesh nylon filter, but similar nanotubes were observed for unfiltered samples (Fig. S5). Transmission electron microscopy (TEM) images show the extensive formation of nanotubes with a monodisperse diameter distribution of 23 nm and a wall thickness of 9 nm (Fig. 3A-C). Cryo-TEM showed the formation of nanotubes that coexist with twisted tapes (Fig. 3D). It could be argued that SucValGlyAzo forms an amphiphilic bilayer that originates a

tape that twists into nanotubes, as reported in related systems.[29,46–48]

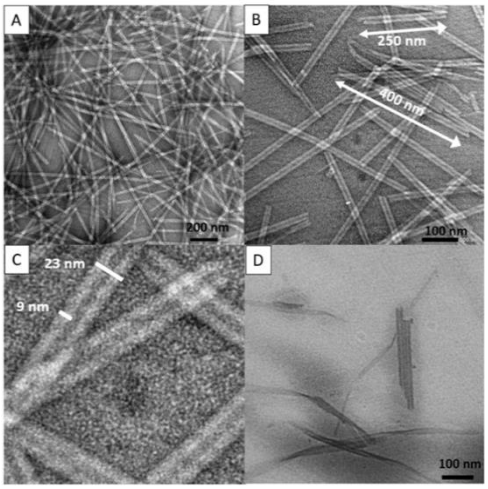

Fig. 3. TEM (A-C) and cryo-TEM (D) images of the nanotubes formed by **SucValGlyAzo** (1.7 mM, 0.1 M Tris buffer, pH 7.4; uranyl acetate was used as a staining agent for the TEM images).

The light-controlled nanotube assembly/diassembly processes were studied by DLS measurements (**Fig. 4**). After UV irradiation, almost no scattering is measured by DLS, revealing that the *trans-cis* isomerization results in nanotube disassembly, with a residual number of aggregates. TEM images (**Fig. S6**) show that most nanotubes have disappeared compared to the images previous to irradiation shown in **Fig. 3**. Noticeably, TEM also reveals that some blurred structures reminiscent of the nanotubes are still present. The thermal equilibration of the system shows that the intensity of scattered light increases with time. Also, after 60 min the size distribution shifts towards smaller apparent diameters. This behaviour can be ascribed to the progressive growth of nanotubes, which in the initial stages are smaller than the residual ones remaining after UV irradiation. Finally, a monomodal size distribution like the initial one, but broader, is achieved after two hours.

The UV-promoted nanotube disassembly can be rationalized considering that *trans*-azobenzene is almost flat and has no dipole moment, whereas the *cis* isomer presents an angular geometry and a dipole moment.[49] This dramatic change would affect intermolecular interactions like aromatic stacking, which are responsible for the self-assembly process.

It is interesting to note that the UV-vis spectra of the sample before UV irradiation and immediately after visible irradiation differ in the shape of the band assigned to the *trans* isomer at ca. 340 nm (**Fig. S7**). Most likely, irradiation with visible lighinitially affords free (non-aggregated) *trans* molecules whose absorption spectrum is more symmetric and slightly red-shifted compared to nanotubes.

The photoisomerization-controlled self-assembly process can also be monitored using the fluorescent probe Nile Red (NR). This dye shows a very weak fluorescence in water that is dramatically boosted upon its incorporation into hydrophobic environments.[50] In the presence of **SucValGlyAzo,** Nile Red shows an intense emission (λ_{max} = 625 nm), indicating the incorporation of the dye in hydrophobic regions of the nanotubes (**Fig. 5** and **Fig. S8**). Irradiation with UV light results in fluorescence quenching and peak shift to 660 nm, indicating the exposition of Nile Red to the aqueous solvent due to light-promoted nanotube disaggregation. Then, irradiation with 457 nm light (30 seconds) provokes a notable fluorescence recovery after 30 min. (Fig. 5).

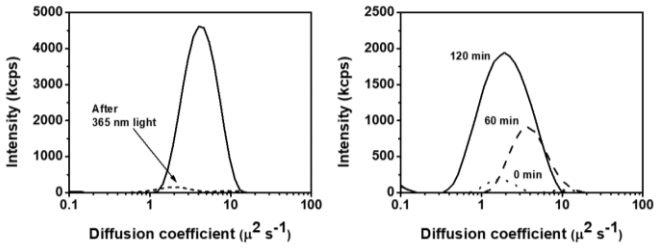

Fig. 4. DLS measurements of a **SucValGlyAzo** solution (1.7 mM, 0.1 M Tris buffer, pH 7.4) Left: Scattering intensity distribution before (solid line) and after (dashed line) irradiation with 365 nm light. Right: Temporal evolution of the scattering intensity distribution for the UV-irradiated sample upon resting in the darkness at 25 ºC.

Summarizing, **SucValGlyAzo** shows photocontrolled reversible self-assembly into nanotubes of monodisperse diameter in aqueous media at physiological pH values. It should be highlighted that **SucValGlyAzo** is a small, synthetically simple molecule. This represents a considerable advantage for envisaged practical applications. Additionally, the reported self-assembly into nanotubes comes from a dipeptide that does not contain a phenylalanine unit. Instead, it seems that the azobenzene unit imparts the required hydrophobic and presumably aromatic stacking interactions for the self-assembly. The blue-shift and broadening observed in the absorption spectrum of the aggregates would support such interactions.

Overall, the reported photocontrolled nanotube formation in water is unprecedented and could constitute a relevant tool for developing smart systems with biomedical applications. For example, UV light-mediated drug delivery can be applied to organs that can be directly illuminated, such as the skin, or to targets that can be reached by endoscopic techniques.[51] Also, this type of system could be used as an actuator to convert light to mechanical work.[52]

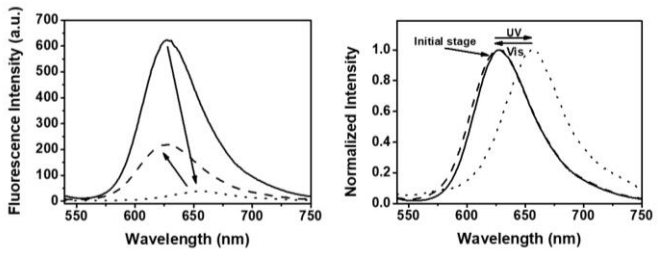

Fig. 5. Emission intensity (λ_{ex} = 520 nm) of a solution of **SucValGlyAzo** containing Nile Red (10 μM). Solid line: initial sample; dotted line: after irradiation with 365 nm light for 30 seconds; dashed line: subsequent irradiation with 457 nm light for 30 seconds and then resting for 30 minutes. Left: Absolute emission intensity. Right: Normalized emission intensity. [**SucValGlyAzo**] = 1.7 mM, 0.1 M Tris buffer, pH 7.4, 25 ºC).

Conflicts of interest

There are no conflicts to declare.

Acknowledgements The authors thank 'Servei Central d'Instrumentació Científica (SCIC) de la Universitat Jaume I'.

Notes and references

1 Z. Fang, Y. Shen and D. Gao, *New J. Chem.*, 2021, **45**, 4534–4544.

2 M. Mamuti, R. Zheng, H.-W. An and H. Wang, *Nano Today*, 2021, **36**, 101036.

3 P. Zhu, R. Chen, C. Zhou, M. Aizenberg, J. Aizenberg and L. Wang, *Adv. Mater.*, 2021, **33**, 202008558.

4 Q. Xiong, Y. Lim, D. Li, K. Pu, L. Liang and H. Duan, *Adv. Funct. Mater.*, 2020, **30**, 1903896.

5 Y. Tao, H. F. Chan, B. Shi, M. Li and K. W. Leong, *Adv. Funct. Mater.*, 2020, **30**, 2005029.

6 Y. Y. Luk and N. L. Abbott, *Curr. Opin. Colloid Interface Sci.*, 2002, 7, 267–275.

7 S. Chen, R. Costil, F. K. C. Leung and B. L. Feringa, *Angew. Chemie - Int. Ed.*, 2021, **60**, 11604–11627.

8 T. Hirose, K. Matsuda and M. Irie, *J. Org. Chem.*, 2006, **71**, 7499–7508.

9 T. Sakata, Y. Yan and G. Marriott, *Proc. Natl. Acad. Sci. U. S. A.*, 2005, **102**, 4759–4764.

10 X. R. Wang, M. P. Li, W. R. Xu and D. Kuck, *Asian J. Org. Chem.*, 2021, **10**, 567–570.

11 Q. Cheng, H. Duan, A. Hao and P. Xing, *ACS Appl. Mater. Interfaces*, 2021, **13**, 2091–2099.

12 A. A. Beharry and G. A. Woolley, *Chem. Soc. Rev.*, 2011, **40**, 4422–4437.

13 X. Xie, L. Wang, X. Liu, Z. Du, Y. Li, B. Li, L. Wu and W. Li, *Chem. Commun.*, 2020, **56**, 1867–1870.

14 S. Yagai, T. Karatsu and A. Kitamura, *Chem. - A Eur. J.*, 2005, **11**, 4054–4063.

15 Y. Q. Nan, J. X. Liu, S. S. Zhang, D. J. Chen, Q. X. Ye, C. Yuan and L. S. Hao, *Colloids Surfaces A Physicochem. Eng. Asp.*, 2020, **601**, 124988.

16 S. H. Nam, Y. J. Choi, Y. W. Kim, K. Jun, N. H. Jeong, S. G. Oh and H. C. Kang, *J. Ind. Eng. Chem.*, 2020, **90**, 203–213.

17 H. C. Kang, B. M. Lee, J. Yoon and M. Yoon, *J. Colloid Interface Sci.*, 2000, **231**, 255–264.

18 H. Sakai, A. Matsumura, S. Yokoyama, T. Saji and M. Abe, *J. Phys. Chem. B*, 1999, **103**, 10737–10740.

19 Y. Wang, P. Han, H. Xu, Z. Wang, X. Zhang and A. V Kabanov, *Langmuir*, 2010, **26**, 709–715.

20 S. Kwangmettatam and T. Kudernac, *Chem. Commun.*, 2018, **54**, 5311–5314.

21 C.-C. Zhang, S.-H. Li, C.-F. Zhang and Y. Liu, *Sci. Rep.*, 2016, **6**, 37014.

22 T. Muraoka, C. Y. Koh, H. Cui and S. I. Stupp, *Angew. Chemie - Int. Ed.*, 2009, **48**, 5946–5949.

23 S. Tamesue, Y. Takashima, H. Yamaguchi, S. Shinkai and A. Harada, *Angew. Chemie - Int. Ed.*, 2010, **49**, 7461–7464.

24 H.-L. Sun, Y. Chen, J. Zhao and Y. Liu, *Angew. Chemie Int. Ed.*, 2015, **54**, 9376–9380.

25 W. Szymański, J. M. Beierle, H. A. V. Kistemaker, W. A. Velema and B. L. Feringa, *Chem. Rev.*, 2013, 113, 6114–6178.

26 X. Song, J. Perlstein and D. G. Whitten, *J. Am. Chem. Soc.*, 1997, **119**, 9144–9159.

27 F.-Q. Li, Q.-L. Yu, Y.-H. Liu, H.-J. Yu, Y. Chen and Y. Liu, *Chem. Commun.*, 2020, **56**, 3907–3910.

28 S. Scanlon and A. Aggeli, *Nano Today*, 2008, **3**, 22–30.

29 C. Valéry, F. Artzner and M. Paternostre, *Soft Matter*, 2011, **7**, 9583–9594.

30 I. W. Hamley, *Angew. Chemie Int. Ed.*, 2014, **53**, 6866–6881.

31 N. Rodríguez-Vázquez, M. Amorín and J. R. Granja, *Org. Biomol. Chem.*, 2017, 15, 4490–4505.

32 X. Yan, P. Zhu and J. Li, *Chem. Soc. Rev.*, 2010, **39**, 1877–1890.

33 E. Gazit, *Chem. Soc. Rev.*, 2007, **36**, 1263–1269.

34 N. Habibi, N. Kamaly, A. Memic and H. Shafiee, *Nano Today*, 2016, **11**, 41–60.

35 S. L. Porter, S. M. Coulter, S. Pentlavalli and G. Laverty, *Macromol. Biosci.*, 2020, **20**, 2000115.

36 M. Johny, K. Vijayalakshmi, A. Das, P. Roy, A. Mishra and J. Dasgupta, *Chem. Commun*, 2017, **53**, 9348.

37 A. A. Deeg, T. E. Schrader, S. Kempter, J. Pfizer, L. Moroder and W. Zinth, *ChemPhysChem*, 2011, **12**, 559–562.

38 Y. Lin, Y. Qiao, P. Tang, Z. Li and J. Huang, *Soft Matter*, 2011, **7**, 2762–2769.

39 M. Fontanillo, C. A. Angulo-Pachón, B. Escuder and J. F. Miravet, *J. Colloid Interface Sci.*, 2013, **412**, 65–71.

40 C. A. Angulo-Pachón and J. F. Miravet, *Chem. Commun.*, 2016, **52**, 5398–5401.

41 D. Navarro-Barreda, C. A. Angulo-Pachón, B. Bedrina, F. Galindo and J. F. Miravet, *Macromol. Chem. Phys.*, 2020, **221**, 1900419.

42 A. Torres-Martínez, C. A. Angulo-Pachón, F. Galindo and J. F. Miravet, *Soft Matter*, 2019, **15**, 3565–3572.

43 P. A. Hassan, S. Rana and G. Verma, *Langmuir*, 2015, 31, 3–12.

44 T. Liu and Z. Xiao, *Macromol. Chem. Phys.*, 2012, **213**, 1697–1705.

45 B. Kang, H. Tang, Z. Zhao and S. Song, *ACS Omega*, 2020, 5, 6229–6239.

46 K. L. Morris, S. Zibaee, L. Chen, M. Goedert, P. Sikorski and L. C. Serpell, *Angew. Chemie - Int. Ed.*, 2013, **52**, 2279–2283.

47 B. Jean, L. Oss-Ronen, P. Terech and Y. Talmon, *Adv. Mater.*, 2005, **17**, 728–731.

48 M. Reches and E. Gazit, *Phys. Biol.*, 2006, **3**, 10–19.

49 J. M. Robertson, *J. Chem. Soc.*, 1939, 232–236.

50 P. Greenspan, E. P. Mayer and S. D. Fowler, *J. Cell Biol.*, 1985, **100**, 965–973.

51 A. Barhoumi, Q. Liu and D. S. Kohane, *J. Control. Release*, 2015, 219, 31–42.

52 J. M. Halabi, E. Ahmed, S. Sofela and P. Naumov, *Proc. Natl. Acad. Sci. U. S. A.*, 2021, **118**, e2020604118.